Structural analysis of the semiconductor-semimetal alloy $Cd_{1-x}Hg_xTe$ by infrared lattice-vibration spectroscopy

S. P. Kozyrev and L. K. Vodopyanov
Lebedev Physics Institute, 117924 Moscow, Russia

R. Triboulet
CNRS Laboratoire de Physique de Solides, Meudon, France

(Received 6 January 1998)

Far-infrared reflectivity measurements have been made on traveling-heater-method-grown $Cd_{1-x}Hg_xTe$ bulk single crystals. The spectra at 300, 77, and 25 K display two bands with fine structure, which cannot be explained by the usual two-oscillator model. These lattice spectra are shown to originate from four Cd-Te and Hg-Te vibrational modes in five basic $Cd(4-n)Hg(n)Te$ $(n=0,1,2,3,4)$ cells consisting of cations tetrahedrally distributed around a shared Te anion. The mode frequencies are determined by the cation configuration in each cell. They are assumed to be independent of alloy composition, which determines only the mode strengths. The temperature dependence of the Cd-Te and Hg-Te vibrations revealed differences. The Cd-Te frequencies decrease with temperature, as is typical for semiconductor compounds. For the Hg-Te vibrations the temperature dependence is more complicated. Such temperature behavior was explained by influence of the anharmonicity corrections, which change sign with variation of frequency. Dispersion analysis of the dielectric function $\varepsilon''(w)$ restored from the reflection spectra of the alloys at 25 K by Kramers-Kronig analysis revealed a peculiarity at 137 cm^{-1}, which appears with nearly constant strength over the wide compositional range $x=0.1-0.8$. This mode has the same temperature dependence as the Cd-Te vibrational modes. The most probable explanation of this mode is associated with the alloy disorder or with multiphonon processes. [S0163-1829(98)02124-9]

I. INTRODUCTION

The discovery by Mikkelsen and Boyce[1] of a bimodal distribution for nearest-neighbor bond lengths in semiconducting $Ga_{1-x}In_xAs$ alloys by EXAFS (extended x-ray absorption fine structure) has rekindled interest in the local structure of semiconductor alloys. X-ray diffraction shows that semiconductor alloys $A_{1-x}B_xC$ with zinc-blende (ZB) structure have a lattice constant $a(x)$ changing linearly with composition x from the lattice constant of compound AC to that of compound BC. In the virtual-crystal approximation it is assumed that the distances between nearest neighbors (that is, the bond lengths) in the alloy are equal to each other and to 0.75 $a(x)$. EXAFS measurements of $Ga_{1-x}In_xAs$ (Ref. 1) and other alloys,[2] however, show local deviations from the ZB structure. Rather than follow the virtual-crystal approximation, the nearest-neighbor distances show a bimodal distribution centered around the bond lengths of the AC and BC compounds. Even when there are large differences in the AC and BC lattice constants, the change in bond lengths in the alloy are only 20–25% of the value predicted by the virtual-crystal approximation. Such a distribution of bond lengths (which is close to the conception of covalent radii conservation[3]) is observed in alloys of covalent III-V compounds,[2] and also in the highly ionic II-VI alloys $Cd_{1-x}Mn_xTe$,[4] $Cd_{1-x}Zn_xTe$,[4] $Hg_{1-x}Mn_xTe$,[5] and $Hg_{1-x}Zn_xTe$.[6] The structural properties of these alloys are explained within the valence force field model,[7,8] in which the relaxation mechanism for the bond lengths is determined primarily by elastic stresses induced by the lattice mismatch of the binary components.

A different situation is obtained in the quasibinary alloy $Hg_{1-x}Cd_xTe$, which forms a continuous series of ZB solid solutions over $x=0-1$. The alloy brings together the semimetal HgTe ($E_g=-0.3$ eV) with covalent and metallic bonding and the wide-gap semiconductor CdTe ($E_g=1.6$ eV), with its combination of covalent and ionic bonding. Both crystallize in the ZB structure, with nearly identical bond lengths, 0.2798 nm for HgTe and 0.2806 nm for CdTe. It is difficult *a priori* to predict the structural behavior and consequently the properties of alloys whose components have the same crystal structure and almost the same lattice parameters—that is, alloys free of lattice-mismatch stresses—but with different types of bonding. Sher *et al.*[9] has used Harrison's tight-binding theory for tetrahedral semiconductors. Later, Hass and Vandberbilt[10] used the pseudopotential method to predict that in the alloy the Hg-Te bond becomes shorter, and the Cd-Te bond becomes longer, which should result in a structural instability. These shifts are attributed to charge transfer from Cd to Hg in the alloy, which changes interionic Coulomb forces. EXAFS measurements[4,5] reveal that the Hg-Te and Cd-Te bond lengths in $Hg_xCd_{1-x}Te$ relax slightly from their values in pure HgTe and CdTe, respectively, changing in opposite directions. Experimental results[11] are used as a basis of calculations of the local relaxation of the bond lengths on the same microscopic model of $Hg_{0.5}Cd_{0.5}Te$ as considered in Ref. 10, but the d-shell electrons in Hg and Cd were regarded as valence electrons similar to the bonding s and p electrons of Hg, Cd, and Te. The authors of Ref. 11 concluded that the ionic charges were governed mainly by the binding between near-

est neighbors and found no evidence for large charge transfers between Cd and Hg in (HgCd)Te alloys—that is, the properties of the nearest-neighbor bonds in pure HgTe and CdTe were retained in the alloy. Wei and Zunger[12] calculated the electron structure of (HgCd)Te from first principles to determine the role of *d* electrons in forming the alloy chemical bonds, and reached similar conclusions.

Magic-angle sample spinning NMR is a new method for investigation of local structure. When it is applied to the cation substitution alloys $Cd_{1-x}Hg_xTe$,[13,14] $Cd_{1-x}Zn_xTe$,[14] and $Cd_{1-x}Mn_xTe$,[14] the chemical shift of the resonance frequency of the Te nuclei is characterized by a set of discrete lines whose number depends on the local composition. The lines are attributed to five possible cation configurations of the form $A(4-n)B(n)$ $(n=0,1,2,3,4)$ around each Te anion. For $Cd_{1-x}Hg_xTe$ with equal Hg-Te and Cd-Te bond lengths that are independent of alloy composition, but with different bond ionicity, the chemical shift is determined by charge transfer between a Te anion and its tetrahedral environment of cations. For each $Cd(4-n)Hg(n)$ configuration, the shift is independent of alloy composition; further, cubic symmetry is retained around Te as alloy composition is varied. NMR data have been used to estimate the degree of cation ordering in $Cd_{1-x}Hg_xTe$. For powder samples of $Cd_{1-x}Hg_xTe$ $(0.1<x<0.9)$,[13,14] the analysis shows some ordering of Hg and Cd at $x=0.25$ and 0.75. But more recently,[15] when the same authors analyzed NMR data from *p*-type as-grown single crystal $Hg_{0.78}Cd_{0.22}Te$, they found that Hg and Cd are randomly distributed

Infrared spectroscopy of the lattice vibrations in $A_{1-x}B_xC$ alloys also gives valuable information about interatomic interactions. Infrared spectra of most ZB or wurtzite III-V and II-VI alloys are characterized by two-mode behavior, where two strong reststrahlen bands appear at frequencies near those of the end-point compounds and that vary weakly with alloy composition, whereas the intensities of the bands are approximately proportional to the concentration of the corresponding compound.[16] Some tetrahedral $(AB)C$ alloys, however, display only a single band, the position of which changes continuously with alloy composition from the TO frequency for one end-point compound to the TO frequency for the other end-point compound, whereas its intensity remains practically constant. According to Refs. 17 and 18 the phonon spectrum behavior of $(AB)C$ alloys is determined by the ratio of the two values: perturbation vibrational energy at the substitution of atom *A* for atom *B*, and interaction vibrational energy of atoms in *AC* lattice. For the two-mode behavior the first energy should be bigger than the second. In the opposite case we have one-mode behavior.

In the anion alloys Ga(AsP) and Cd(SeS), fine structure atop the main infrared reflectivity bands has been explained by assuming a nonrandom distribution of anions of different sorts around the common cation.[19,20] Infrared spectra for the cation alloy $Cd_{1-x}Hg_xTe$ also show considerable fine structure, which has been attributed to a formation of short-range clusters.[21] A cluster model of distribution of the anions around the common cation considered by Verleur and Barker[20] for the alloys Cd(SeS) was used by Perkowitz, Kim, and Becla[22] to analyze ir reflection spectra of $CdSe_xTe_{1-x}$ $(x=0.05-0.35)$ at 80 K. This model was also used for the comparison of cluster effect in the anion alloys Cd(SeTe) and Cd(SeS). Similarly, it was not possible to reproduce reflectivity spectra from $Cd_{1-x}Zn_xTe$ $(x=0.005-0.50)$ at 20 K (Ref. 23) using only two modes, a CdTe- and a ZnTe-like vibration.

In this paper, we present analysis and interpretation of infrared lattice reflection spectra from $Cd_{1-x}Hg_xTe$ $(0<x<0.8)$, which agrees with the latest investigations of local structure of semiconductor alloys. We measured spectra at temperatures as low as 25 K, and analyzed them by successive applications of dispersion and Kramers-Kronig (KK) methods, to clearly reveal band details. The lattice spectra of $Cd_{1-x}Hg_xTe$ are shown to originate from four each Cd-Te and Hg-Te vibrational modes in five basic $Cd(4-n)Hg(n)Te$ $(n=0,1,2,3,4)$ cells consisting of cations tetrahedrally distributed around a shared Te anion. The mode frequencies are determined by the cation configuration in each cell. They are assumed to be independent of alloy composition, which determines only the mode strengths. Analysis of strength vs alloy composition provides information on the relative content of the basic cells at that composition and, consequently, on the nature of the cation substitutions.

II. MEASUREMENT AND ANALYSIS OF LATTICE REFLECTION SPECTRA

Single crystals of $Cd_{1-x}Hg_xTe$ $(0<x<0.8)$ were grown with a traveling-heater method (THM).[24] Among different methods of $Hg_xCd_{1-x}Te$ bulk crystal growth the THM, combining some advantages of solution growth and zone melting with those of the growth under steady-state condition, is the most promising method. This method allowed us to grow pure homogeneous oriented crystals of large dimensions. Ingots of 30 mm diameter and up to 80 mm in length were currently produced with longitudinal homogeneity better than ± 0.02 mol and radial homogeneity better than ± 0.002 mol for $x=0.21$, 0.3, and 0.7. Electron carrier concentration of 2×10^{14} cm^{-1} with mobility of 160 000 cm^2/V s at 77 K for $x=0.21$, as well as the high performance of photoconductor detectors, such as R_0A product of 16 Ω cm^2 at 77 K, for crystals with $x=0.21$, attest to the high quality of the grown crystals.[24] The reflection spectra of these samples were determined at temperatures of 25, 85, and 300 K, using a vacuum diffraction spectrometer that covered the range 110–250 cm^{-1} at a resolution of 1 cm^{-1}. At each wavelength, the reflection from the sample and from a reference mirror was measured consecutively at the same location on the sample.

Figure 1 shows the reflection spectra of $Cd_{0.29}Hg_{0.71}Te$ at 25, 85, and 300 K. Two strong reflectivity bands are observed at frequencies that vary little with alloy composition *x*. As *x* increases, the high-frequency CdTe-like band becomes weaker, departing from the value for pure CdTe; and the low-frequency HgTe-like band strengthens approaching the value for pure HgTe. In the range $x=0.1-0.6$ fine structure appears near the CdTe-like vibrations. This structure was also observed for $x=0.71$ and 0.80 at the lower temperature of 25 K. These spectra cannot be interpreted solely in terms of a simple two-mode model, with one each of a CdTe-like and HgTe-like vibrational mode. For deeper analysis, we processed the spectra by successive applications of dispersion analysis and Kramers-Kronig analysis to deter-

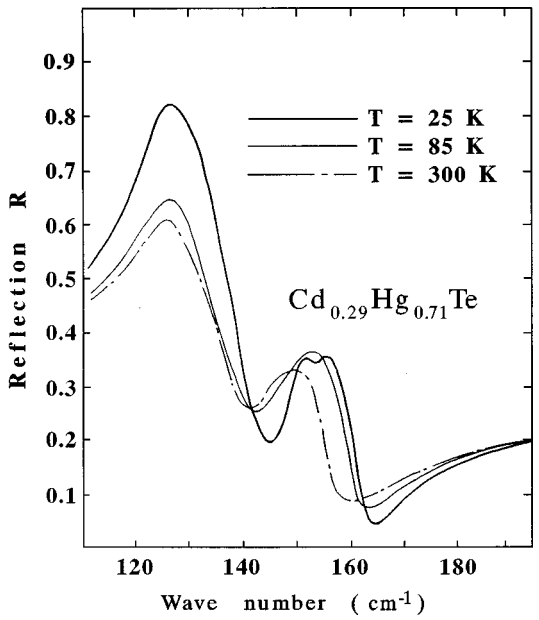

FIG. 1. Reflection spectra $R(\omega)$ of $Cd_{0.29}Hg_{0.71}Te$ at $T=25$, 85, and 300 K.

mine the complex dielectric function $\hat{\varepsilon}(\omega)=\varepsilon'(\omega)+i\varepsilon''(\omega)$. The KK method is independent of the form of $\hat{\varepsilon}(\omega)$, since it involves only the complex reflection amplitude $\hat{r}=r(\omega)\exp(iq)$. It can in principle identify all the significant oscillators that generate the reflectivity spectrum, without the need to arbitrarily insert any oscillator *a priori*. However, the integral transform at the heart of the KK method is sensitive to boundary conditions, since we can measure $r(\omega)$ only over a finite frequency interval. Our combination of dispersion and KK analysis is designed to correctly elicit all the structure inherent in the reflectivity spectra, by extending $\hat{r}(\omega)$ outside the measured frequency range through the use of oscillators with parameters calculated by dispersion analysis.

In the first stage of our processing we approximated the infrared response of the alloy by equating $\hat{\varepsilon}(\omega)$ to the sum of two Lorentzian oscillators corresponding to HgTe-like and CdTe-like TO vibrations,

$$\hat{\varepsilon}(\omega)=\varepsilon_\infty+\Sigma\,\frac{S_j\omega_j^2}{\omega_j^2-\omega^2-i\omega\Gamma_j}. \tag{1}$$

We selected the oscillator parameters ω_j, S_j, and Γ_j to yield a model spectrum that approximated the measured reflectivity and extended it to frequencies outside our experimental values. Then we used the extended data to reconstruct $\hat{\varepsilon}(\omega)$ through KK analysis. This yielded additional structure beyond that from the two original oscillators. In the second step, the imaginary dielectric function $\varepsilon''(\omega)$ obtained from the KK transformation was expanded into a set of oscillators, whose parameters were then optimized to match the measured reflectivity spectrum. Then this model spectrum that closely approximated the experimental reflectivity was used outside the measured frequency interval to determine the final form of $\hat{\varepsilon}(\omega)$ by KK analysis. The results of this mathematical processing are a model reflection spectrum that can be compared to the experimental one; and a model dielectric

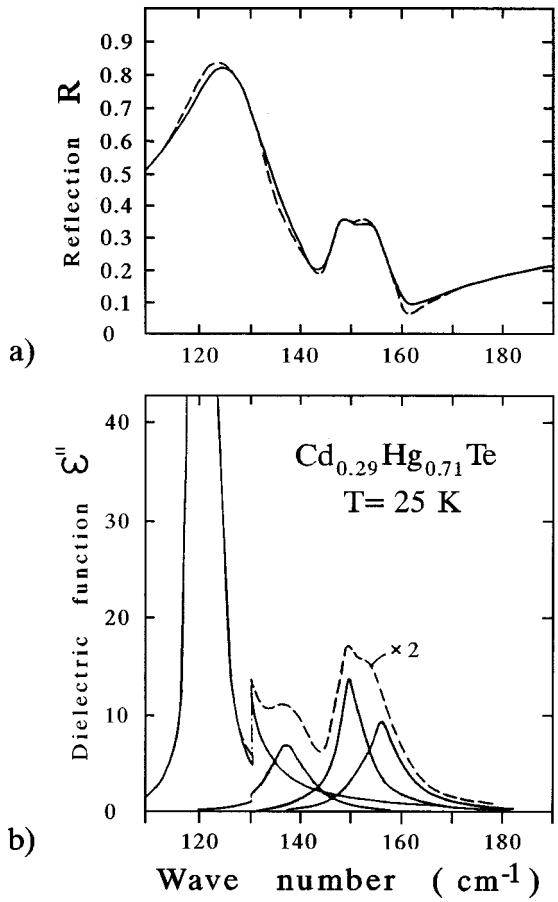

FIG. 2. (a) Reflection spectra $R(\omega)$ of $Cd_{0.29}Hg_{0.71}Te$ at $T=25$ K (the dashed curve represents the experimental spectrum and the continuous curve is the model spectrum); (b) the dielectric function $\varepsilon''(\omega)$ (dashed curve) reconstructed by the Kramers-Kronig analysis of the $R(\omega)$ spectrum, and the Lorentzian profiles (continuous curves) of the harmonic oscillators into which the function $\varepsilon''(\omega)$ is expanded.

function $\hat{\varepsilon}(\omega)=\varepsilon'(\omega)+i\varepsilon''(\omega)$, along with a set of parameters defining its oscillators. Peaks in the spectral distribution of $\varepsilon''(\omega)$ correspond to the frequencies of the TO modes, whereas the peaks in $\mathrm{Im}[-1/\hat{\varepsilon}(\omega)]$ lie at the frequencies of the longitudinal (LO) modes.

III. RESULTS

A. Alloys rich in HgTe: $Cd_{0.29}Hg_{0.71}Te$ and $Cd_{0.19}Hg_{0.81}Te$

Figure 2 shows $\varepsilon''(\omega)$ (dashed curve) as reconstructed by KK analysis of the reflection spectrum of $Cd_{0.29}Hg_{0.71}Te$ at 25 K, and the corresponding expression that uses damped Lorentzian harmonic oscillators (continuous curves). There are two well-resolved oscillators at 150.5 and 156 cm^{-1} with strengths of 0.25 and 0.20, respectively, which are the CdTe-like lattice modes. HgTe-like vibrations appear as a single strong mode at 121.5 cm^{-1} with a large strength of 4.7. The 137-cm^{-1} mode, whose strength of 0.25 is comparable to those of the CdTe-like modes, was detected in $\varepsilon''(\omega)$. This mode is hidden in the reflection spectrum, even at 25 K, because it lies in the wing of the very strong HgTe-like band. The data also give LO frequencies of 142.0 cm^{-1} for the

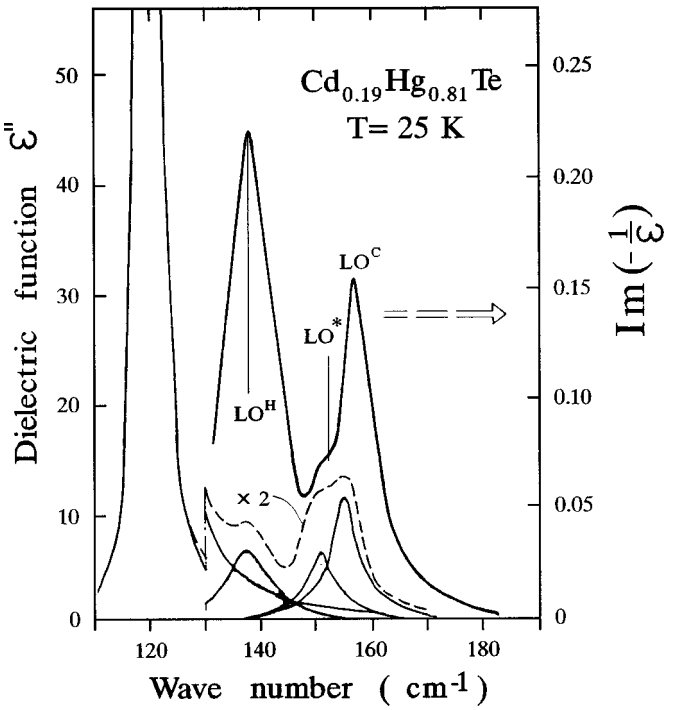

FIG. 3. Dielectric function $\varepsilon''(\omega)$ (dashed curve) of $Cd_{0.19}Hg_{0.81}Te$ at $T=25$ K reconstructed by the KK analysis of the $R(\omega)$ spectrum, and the Lorentzian profiles (continuous curves) of the harmonic oscillators into which the function $\varepsilon''(\omega)$ is expanded. The figure gives also $\mathrm{Im}[-\hat{\varepsilon}(\omega)^{-1}]$ (upper continuous curves).

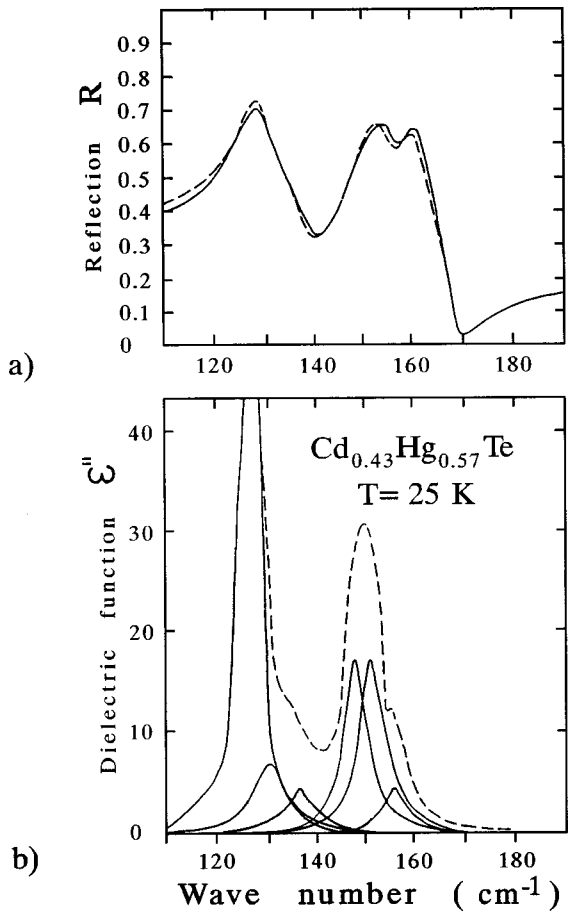

FIG. 4. (a) Reflection spectra $R(\omega)$ of $Cd_{0.43}Hg_{0.57}Te$ at $T=25$ K (the dashed curve is the experimental spectrum and the continuous curve is the model spectrum); (b) the dielectric function $\varepsilon''(\omega)$ (dashed curve) reconstructed by the KK analysis of the $R(\omega)$ spectrum, and the Lorentzian profiles (continuous curves) of the harmonic oscillators into which the function $\varepsilon''(\omega)$ is expanded.

HgTe-like TO vibration (at 121.5 cm^{-1}), and 155 and 161.0 cm^{-1} for the CdTe-like TO vibrations (at 150.5 and 156 cm^{-1}).

A similar analysis for $Cd_{0.19}Hg_{0.81}Te$ (Fig. 3) gives TO frequencies of 121.0 cm^{-1} for the HgTe-like vibration and 151.0 and 155.5 cm^{-1} for the CdTe-like vibrations, which agree to within 0.5 cm^{-1} with other results.[25] The LO frequencies are 139.5 cm^{-1} for the HgTe-like vibration, and 153 and 158.5 cm^{-1} for the CdTe-like vibrations. In Ref. 25 the LO mode at 158 cm^{-1} was paired with the TO mode at 151 cm^{-1}, but we disagree. According to our analysis, the CdTe-like band in the reflection spectrum is governed by TO modes at 151.0 and 155.5 cm^{-1} with strengths 0.12 and 0.23, respectively. They correspond to LO modes at 153 and 158.5 cm^{-1} with LO-TO splittings of 2 and 3 cm^{-1}, respectively. The LO mode observed at 156 cm^{-1} in the Raman spectra[25] is probably an average of these values because the two LO modes are unresolved; or may involve the TO mode at 155.5 cm^{-1}, which appears because lattice disorder relaxes the ordinary selection rule. The 137-cm^{-1} mode we observe in Lorentzian profiles derived from $\varepsilon''(\omega)$ has an oscillator strength comparable to that of the CdTe-like TO modes. The mode at 135 cm^{-1} had been observed for $Hg_{0.8}Cd_{0.2}Te$ in resonance Raman scattering (RRS) spectra at liquid-nitrogen temperatures.[26] On the basis of calculations of the phonon state density, it has been attributed[27] to vibrations of the Te atom bound tetrahedrally to one Cd atom and three Hg atoms. The same interpretation is adopted in Ref. 25 to explain a 137-cm^{-1} mode uncovered through KK analysis of the reflection spectrum of $Hg_{0.79}Cd_{0.21}Te$ at 10 K, and also in Ref. 28 to explain a mode at 133 cm^{-1} observed in RRS from $Cd_{1-x}Hg_xTe$ with $x=0.69-0.80$ at 80 K.

B. Alloys of intermediate composition: $Cd_{0.43}Hg_{0.57}Te$ and $Cd_{0.48}Hg_{0.52}Te$

The lattice reflection spectra of $Cd_{1-x}Hg_xTe$ with x near 0.5 also cannot be fully described by a two-mode model. Figure 4 shows $\varepsilon''(\omega)$ (dashed curve) at 25 K, from KK analysis, and its expansion into Lorentzian oscillators (continuous curve). The spectrum is similar to that shown in Fig. 2; only the oscillator strengths of the lattice modes are different. For $Cd_{0.43}Hg_{0.57}Te$, $\varepsilon''(\omega)$ is strongly asymmetric near the HgTe-like vibrations. Servoin and Gervais[29] note that such asymmetry may arise from two close-spaced modes with different strengths (or from anharmonic effects, which we do not expect at our low measurement temperature of 25 K). The $\varepsilon''(\omega)$ spectrum near the HgTe-like vibrations can be expanded into two lattice vibration modes; one at 126.5 cm^{-1} with oscillator strength 2.2 and one at 131.0 cm^{-1} with strength 0.45. The CdTe-like vibrations are characterized by three modes at 148.5, 150.5, and 156.6 cm^{-1}. Once again, $\varepsilon''(\omega)$ has a singularity at 137.5 cm^{-1} with oscillator strength 0.25. We show later that

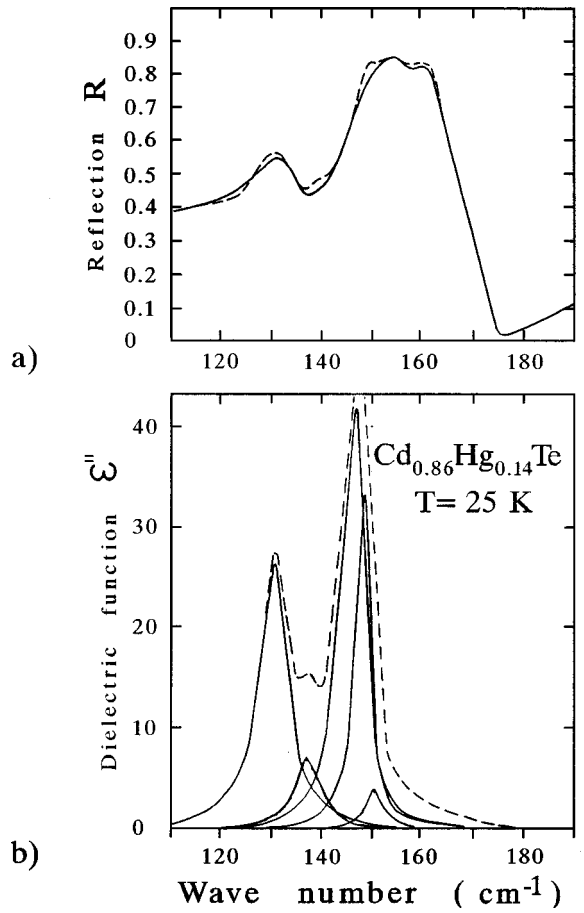

FIG. 5. (a) Reflection spectra $R(\omega)$ of $Cd_{0.86}Hg_{0.14}Te$ at $T=25$ K (the dashed curve is the experimental spectrum and the continuous curve is the model spectrum); (b) the dielectric function $\varepsilon''(\omega)$ (dashed curve) reconstructed by the KK analysis of the $R(\omega)$ spectrum, and the Lorentzian profiles (continuous curves) of the harmonic oscillators into which the function $\varepsilon''(\omega)$ is expanded.

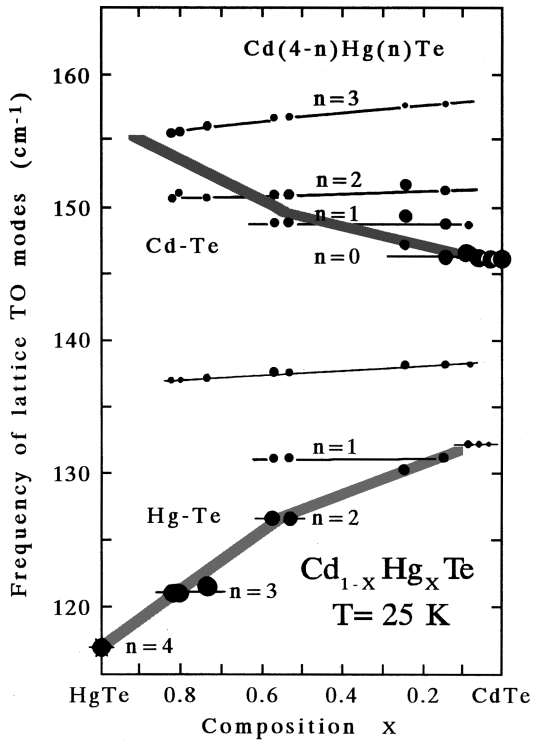

FIG. 6. Distribution of the frequencies of the lattice TO modes ω_n^C and ω_n^H of, respectively, the Cd-Te and Hg-Te vibrations of the basic Cd(4-n)Hg(n)Te cells ($n=0,1,2,3,4$) as a function of the composition of $Cd_{1-x}Hg_xTe$ alloys at $T=25$ K. The figure also shows by wide strips, the distribution of the positions of maxima of the dielectric function $\varepsilon''(\omega)$ of $Cd_{1-x}Hg_xTe$ alloys (reconstructed by the Kramers-Kronig analysis of the reflection spectrum), which correspond to the frequencies of TO modes of CdTe and HgTe-like vibrations in accordance with the two-mode approximation for the vibrational spectra of alloys.

this singularity appears with almost the same strength in $Cd_{1-x}Hg_xTe$ with composition $x=0.09-0.81$. Therefore, unlike the statement in Ref. 25, there is no reason to regard it as only typical of alloys with $x=0.7-0.8$, corresponding to vibrations of the Te atom in the tetrahedron consisting of one Cd atom and three Hg atoms.

C. Alloys rich in CdTe: $Cd_{0.76}Hg_{0.24}Te$ and $Cd_{0.86}Hg_{0.14}Te$

The reflection spectra of CdTe-rich $Cd_{1-x}Hg_xTe$ are more complex than those of the HgTe-rich alloy. They exhibit one HgTe-like TO mode, two CdTe-like TO modes, and a singularity at 137 cm^{-1}. Figure 5 shows the spectrum for $Cd_{0.86}Hg_{0.14}Te$, at 25 K. One HgTe-like TO mode appears in $\varepsilon''(\omega)$ at 131 cm^{-1}. Near the CdTe-like vibrations, we expanded $\varepsilon''(\omega)$ into Lorentzian oscillators with frequencies 146.0, 148.5, and 151.0 cm^{-1}. A singularity also appeared at 138 cm^{-1} in the CdTe-rich alloy, and with the same oscillator strength, 0.3, seen for HgTe-rich alloys; again, this singularity is not limited to alloys with $x=0.7-0.8$. The expansion of $\varepsilon''(\omega)$ into its Lorentzian profiles does not show an additional oscillator of strength 0.02 at 157.5 cm^{-1} because it is difficult to resolve. However, this weak oscillator with a frequency near the LO-TO splitting of the strong CdTe-like vibrations manifests itself in a well-defined dip at the top of the CdTe-like reflection band. The TO phonon frequencies corresponding to the oscillators in the dispersion analysis of $\varepsilon''(\omega)$ and the reflection spectrum $R(\omega)$ of the $Cd_{1-x}Hg_xTe$ alloys for $x=0$ to $x=0.81$ at 25 K (Figs. 2–5), are plotted in Fig. 6. The size of the points in the figure corresponds to the mode oscillator strengths. The frequency 117 cm^{-1} of the TO mode of HgTe at 8 K was taken from Ref. 30. This figure illustrates a main point in our analysis: at all compositions, all the measured frequencies for the CdTe-like vibrations of (CdHg)Te lie within 1 cm^{-1} of four modes: 146, 148.5, 150.5, and 156 cm^{-1}. At any composition the CdTe-like vibrations are governed by four lattice modes with frequencies approximately independent of composition, which alters only the oscillator strengths of these modes.

IV. DISCUSSION

A. Lattice modes of Cd-Te and Hg-Te vibrations

To discuss our observations, we begin with the cases of one-mode and two-mode behavior. According to the work of Onodera and Toyozawa[17] we have one-mode behavior when the perturbation energy at the substitution of one atom by another is smaller than the exchange energy. As has been shown by Dow *et al.*[18] for the case of phonons the perturba-

tion has the form $|\Delta m|\Omega^2$, where Δm is the change of mass, Ω is the frequency of the order of a local or gap mode, and the exchange term is equal to the force constant K. Thus for one-mode behavior we have $|\Delta m|\Omega^2 < K$, and two-mode behavior is realized when the opposite inequality holds. If the inequality is not strong, that is, $|\Delta m|\Omega^2$ is close to K, the mixed cases can be realized, when we have one-mode behavior in one part of the alloy composition, and two-mode behavior in the another. One-mode behavior is characteristic of solid solutions of ionic alkali halide compounds, and two-mode behavior is seen in heavily covalent III-V and II-VI binary compounds that crystallize in the zinc-blende or wurtzite structure. Verleur and Barker[19] have departed from the two-mode concept to explain spectra from $GaAs_yP_{1-y}$, which are of the two-mode type, but with additional structure on each band. They extended the random element isodisplacement model with three coordinates for As, P, and Ga, which gives two TO modes (and an acoustic mode) by adding 13 coordinates that allow for the three-dimensional structure of the alloy; and by assuming that the As and P atoms are not randomly distributed in the anion sublattice, but form clusters consisting of one type of atom. It is remarkable that with sufficiently strong clustering, two of the 12 optical modes (one of the 13 modes is acoustic) dominate at all compositions to give the two main bands, whereas the weaker modes determine the additional spectral structure. However, the Verleur-Barker (VB) scheme has some drawbacks. It is well known that in a disordered lattice, in particular, in $A_{1-x}B_xC$ alloys, because of the selection rules relaxation over a wave vector k, that nearly all of $6N$ modes are optical active. In the VB model only 13 modes are regarded. Therefore this model cannot describe, on a microscopic level, the broadening of the optical-active phonons, because this process is due to the interaction with $k \neq 0$ modes. From this model it is also impossible to calculate the phonon density of states.

We first reported[21] a similar interpretation we used to analyze $Cd_{1-x}Hg_xTe$ lattice reflection spectra at $T = 85$ K. Our spectra were characterized by two strong bands at frequencies that vary little with composition, but samples with $x = 0.1-0.6$ exhibit clear additional structure near the CdTe-like band. The existence of fine structure in the reflection spectra was regarded as a manifestation of clustering in the alloys. The four-mode distribution of CdTe-like oscillators for all compositions agrees with the five basis cells microstructure model. In view of the predominantly covalent nature of the bonding in tetrahedral compounds, in the first approximation we ignore interactions among the basis cells. Then we can derive alloy properties by averaging over the cells, weighted by the probability function $P(x)$ that represents the distribution of the different types of cells at a given composition. Using this approach, Wei and Zunger[12] have calculated from first principles the electronic structure of $Cd_{1-x}Hg_xTe$, and the authors of Refs. 13–15 have interpreted fine NMR structure from ^{125}Te nuclei in the cation alloys $Hg_{1-x}Cd_xTe$,[13–15] $Cd_{1-x}Zn_xTe$,[14] and $Cd_{1-x}Mn_xTe$.[14]

Figure 7 shows the $Cd(4-n)Hg(n)Te$ tetrahedral basis cells with $n = 0$, 1, 2, 3, and 4. Each configuration supports one Cd-Te vibrational mode and one Hg-Te vibrational mode, except that there is no Hg-Te mode at $n = 0$, and no Cd-Te mode at $n = 4$. Thus the five-cell configurations exhibit among them four Cd-Te modes at frequencies ω_n^C and four Hg-Te modes at frequencies ω_n^H.

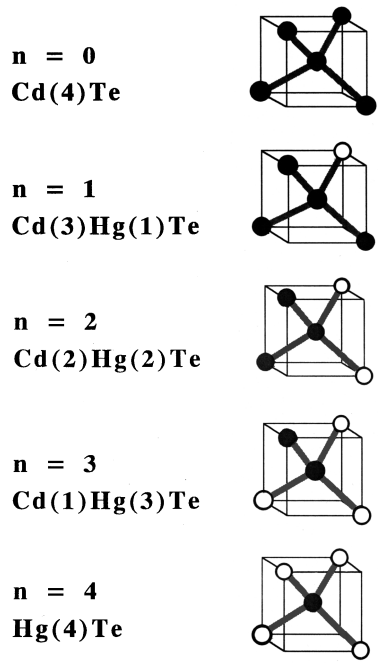

FIG. 7. Tetrahedral $Cd(4-n)Hg(n)Te$ basic cells with $n = 0,1,2,3,4$ of $Cd_{1-x}Hg_xTe$ alloys.

For $Cd_{1-x}Hg_xTe$ formed from binary CdTe and HgTe with almost identical bond lengths (2.806 and 2.798 Å, respectively), EXAFS (Refs. 4 and 5) shows that the Cd-Te and Hg-Te bond lengths remain the same as in the binary compounds for any composition; nor does the dimension of the basis cells change. Hence, there is no reason why local stresses should appear as composition changes. Another hypothesis,[9,10] that the charge between the Cd and Hg atoms becomes redistributed as composition changes, also remains unconfirmed.[11,12] For $Cd_{1-x}Hg_xTe$ at 25 K it follows from Fig. 6 that the Cd(4)Te ($n = 0$) basis cell has a Cd-Te vibrational mode of frequency $\omega_0^C = 146\ cm^{-1}$, whereas the Cd(3)Hg(1)Te ($n = 1$) cell has a mode with $\omega_1^C = 148.5\ cm^{-1}$, the Cd(2)Hg(2)Te ($n = 2$) cell has a mode with $\omega_2^C = 150.5\ cm^{-1}$, the Cd(1)Hg(3)Te ($n = 3$) cell has a Cd-Te vibrational mode of frequency $\omega_3^C = 156\ cm^{-1}$.

For CdTe-rich $Cd_{1-x}Hg_xTe$ we can identify either three or four CdTe-like lattice modes, whereas for HgTe-rich $Cd_{1-x}Hg_xTe$, only one HgTe-like mode appears, and two modes are exhibited only for the intermediate compositions $x = 0.52$ and $x = 0.57$ (Fig. 6). The different Cd-Te and Hg-Te chemical bonds determine their mode behaviors.

In a model calculation[31] of the lattice vibration frequencies for an ''ideal'' $A_{1-x}B_xC$ alloy with atomic parameters corresponding to $Cd_{1-x}Hg_xTe$, we obtained agreement between the calculated distribution of the vibration frequencies for alloys with different composition, and the discrete set of frequencies of the Cd-Te and Hg-Te lattice vibrations for $Cd_{1-x}Hg_xTe$, determined from the ir lattice reflection spectra (Fig. 8). The only discrepancy was that in the BC-rich $A_{1-x}B_xC$ alloys the BC-like vibrations are characterized by a number of ir-active vibrational modes [Fig. 8(a)] but for

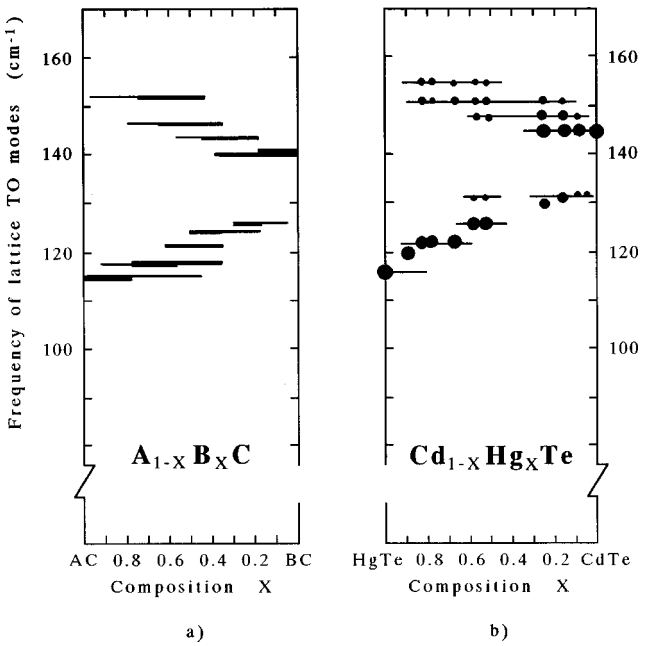

FIG. 8. (a) Distributions of the frequencies of the ir-active vibrations plotted as functions of the composition x of $A_{1-x}B_xC$ alloys, calculated in the rigid-ion approximation for an ''ideal'' alloy with the atomic parameters of the $Cd_{1-x}Hg_xTe$ alloy. (b) Distribution of the frequencies of the optical modes of the lattice vibrations, plotted as a function of the composition x of a $Cd_{1-x}Hg_xTe$ alloy, deduced from an analysis of the far ir reflection spectra.

the $Cd_{1-x}Hg_xTe$ alloys, there is only a single mode [Fig. 8(b)]. We believe that this single mode is only apparent, however, because the vibrations associated with the Hg-Te bond are not truly independent. When modes are coupled and strongly damped, the normal-mode frequencies tend to approach each other, as shown, for instance, in a classical analysis by Barker and Hopfield.[32] If the difference between mode frequencies is comparable to or less than the damping parameter, they appear as a single mode as they interact with infrared radiation. We believe the two or three strongest Hg-Te modes are sufficiently coupled and damped, via anharmonic interaction, to appear as an apparently single Hg-Te oscillator. The frequency of that apparent single mode, as determined from dispersion analysis of the reflection spectra, is the average of the frequencies of the strongest modes. In correspondence with these comments, we assign the strong mode of the Hg-Te vibrations with $\omega_3^H = 121\ \mathrm{cm}^{-1}$ observed at $x=\frac{3}{4}$ to the Cd(1)Hg(3)Te basis cell. For CdTe-rich alloys with $x=0.03$, 0.06, and 0.09, the gap mode at 132 cm^{-1} is observed, which for $x=0.14$ and 0.24, goes into the lattice mode of the Hg-Te vibrations with $\omega_1^H = 131\ \mathrm{cm}^{-1}$ corresponding to the Cd(3)Hg(1)Te basis cell. For intermediate compositions $x=0.52$ and 0.57 there are two Hg-Te modes, corresponding to the Cd(3)Hg(1)Te basis cell with $\omega_1^H = 131\ \mathrm{cm}^{-1}$, and the Cd(2)Hg(2)Te cell with $\omega_2^H = 126\ \mathrm{cm}^{-1}$.

The temperature dependence of the Cd-Te and Hg-Te mode frequencies for the Cd$(4-n)$Hg(n)Te basis are of interest. The Cd-Te frequencies decrease by 5 cm^{-1} as temperature increases from 25 to 300 K, typical semiconductor behavior. However, the metallic binding in HgTe is manifested by an anomalous temperature dependence of the HgTe vibrational modes. As temperature increases from 8 to 300 K, the optical mode frequency increases from 117 to 119 cm^{-1},[29] and the mode frequency of the Cd(1)Hg(3)Te basis cell increases by 2 cm^{-1}. However, the Hg-Te mode of the Cd(3)Hg(1)Te cell behaves like an ordinary semiconductor mode; its frequency decreases from 131 to 128 cm^{-1} as temperature increases. In CdTe-rich $Cd_{1-x}Hg_xTe$, dominated by Cd(4)Te and Cd(3)Hg(1)Te cells, the individual Hg-Te bonds are semiconductorlike; but in HgTe-rich alloys dominated by Hg(4)Te, Cd(1)Hg(3)Te, and Cd(2)Hg(2)Te basis cells, the Hg-Te bonds behave anomalously. The temperature dependence of the phonon mode frequencies are determined by two factors. First is the lattice expansion as the temperature increases, which leads to the decreasing of the frequency with temperature. Second is connected with the anharmonicity corrections to the mode frequency ω:

$$\Delta\omega = \frac{1}{\pi}\int \frac{\gamma(\omega)d\omega}{\omega-\omega'} = \frac{1}{\pi}\frac{\gamma(\overline{\omega})\overline{\omega}}{\omega-\overline{\omega}},$$

where $\gamma(\omega)$ is the damping function of the mode ω, connected with anharmonicity $\gamma(\omega)T$. From the above equation it is clear that $\Delta\omega$ can have a different sign depending on the position of the ω mode relative to the ''center of gravity'' of the combinational frequencies $\overline{\omega}$. From the comparison of phonon dispersion curves for CdTe and HgTe it is seen that for CdTe the acoustical branches are close to the optical branches (the gap is small), whereas for HgTe the acoustical branches are shifted towards the low-frequency region. Therefore we can assume that, for $\omega=\omega_{\mathrm{TO}}$ for CdTe and for close frequencies in $Hg_xCd_{1-x}Te$ alloy, the situation is realized when $\omega<\overline{\omega}$. For similar frequencies for HgTe and the alloy we have the reverse case, $\omega>\overline{\omega}$. Thus the different temperature behavior of TO modes in CdTe and HgTe ranges can be explained by different signs of the anharmonicity corrections.

B. Oscillator strengths of Cd-Te and Hg-Te lattice vibrational modes

Figure 9 shows the oscillator strengths S_n^C vs x derived from our dispersion analysis of the Cd-Te modes corresponding to the Cd$(4\text{-}n)$Hg(n)Te basis cells ($n=0,1,2,3$) at 25 K. A given mode frequency represents a given type of basis cell with a definite cation configuration, whereas the oscillator strength of that mode represents the fraction of cells with that configuration. For a random uncorrelated distribution of Cd and Hg atoms in the cation sublattice of $Cd_{1-x}Hg_xTe$ of composition x, the probability of finding a basis cell with (n)Hg atoms and $(4\text{-}n)$Cd atoms around a shared Te atom is

$$P_n(x) = \binom{4}{n}(1-x)^{4-n}x^n, \tag{2}$$

where

$$\binom{4}{0} = \binom{4}{4} = 1, \quad \binom{4}{1} = \binom{4}{3} = 4, \quad \binom{4}{2} = 6.$$

Noting that the fraction of the Hg atoms in the Cd$(4\text{-}n)$Hg(n)Te basis cell out of four cations represents

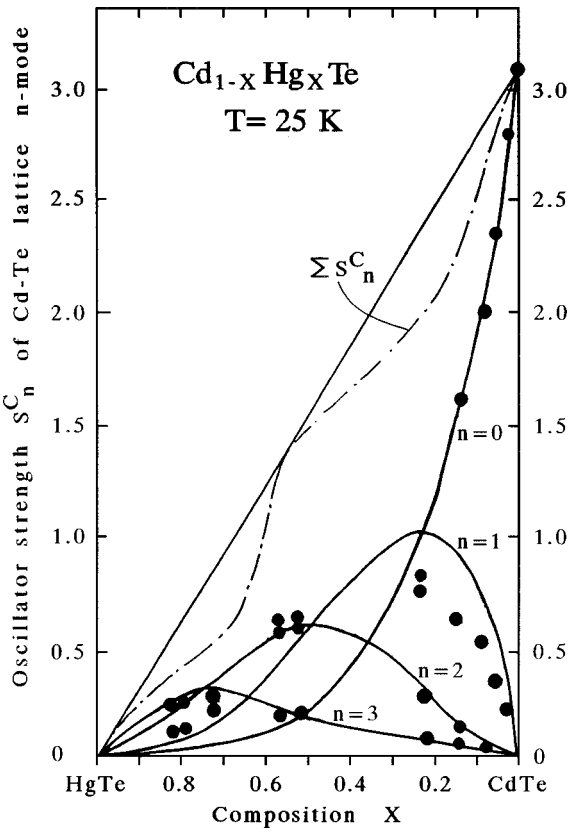

FIG. 9. Oscillator strengths S_n^C of Cd-Te lattice vibrational modes in Cd(4-n)Hg(n)Te basic cells plotted for different compositions of $Cd_{1-x}Hg_xTe$ alloys at $T=25$ K. The continuous curves give the distributions of the oscillator strength $S_n^C(x)$ for four modes with $n=0$, 1, 2, and 3, as a function of the alloy composition using the approximation of a random distribution of Cd and Hg cations in the alloy.

$\alpha_n=n/4$, the probability $P_n^H(x)$ that the Hg atoms in an alloy of composition x are in these cells amounts to

$$P_n^H(x)=\alpha_n P_n(x)=\frac{n}{4}\binom{4}{n}(1-x)^{4-n}x^n, \tag{3}$$

and similarly for Cd atoms, we have the corresponding probability

$$P_n^C(x)=(1-\alpha_n)P_n(x)=\frac{4-n}{n}\binom{4}{n}(1-x)^{4-n}x^n. \tag{4}$$

For a system of independent lattice vibrations the oscillator strength S_n^C of nth lattice mode of the Cd-Te vibrations is

$$S_n^C(x)=f_n^C N P_n^C(x), \tag{5}$$

where f_n^C is the oscillator strength per Cd-Te bond, N is the total number of cations (or ion pairs) in the alloy per unit volume, and $NP_n^C(x)$ is the probable number of Cd cations per unit volume in an alloy of composition x in cells with the Cd(4-n)Hg(n)Te configuration. For pure CdTe ($x=0$, $n=0$), with a measured oscillator strength of 3.1, $S_0^C(x)=3.1P_0^C(x)=3.1(1-x)^4$ for the Cd(4) configuration. Had the reduced oscillator strength f_n^C been independent of the configuration of the Cd(4-n)Te(n)Te cell and amounted to f_0^C, for the oscillator strength of the rest of basis cells Eq. (5) would have reduced to $S_n^C(x)=3.1P_n^C(x)$. The oscillator strengths $S_n^C(x)$ for the CdTe modes with $n=0$, 1, 2, 3 vs composition are shown in Fig. 9 by continuous curves. Their total oscillator strength is described by a linear dependence on the composition $S^C(x)=\Sigma S_n^C(x)=f_0^C N\Sigma P_n^C(x)=3.1(1-x)$. However, the experimental values of the total oscillator strengths of four Cd-Te vibrations, represented by the chain curve in Fig. 9, deviate appreciably from a linear dependence on the composition, with the greatest deviations at $x=0.25$ and 0.75. Such deviation may be explained either by a cluster effect,[19] connected with nonrandom distribution of different cation configurations of the basis cells in $Cd_{1-x}Hg_xTe$,[21] or by the dependence of f_n^C on the configuration of the basis cell, associated with charge transfer. In this case one can expect a correlation between f_n^C and ω_n^C vs the basis cell number n. The four frequencies, attributed to CdTe-like TO modes associated with the basis cells $n=0$, 1, 2, 3, are 146, 148.5, 150, and 156 cm^{-1}. Note that the differences between these frequencies, 5.5, 2, and 2.5, do not vary in a way consistent with the expectations of a simple elastic spring model. However, for a sequence of the experimental mode strengths ($f_1^C=3.1$, $f_2^C=2.4$, $f_3^C=3.2$, and $f_4^C=2.8$) there is no clear correlation with a sequence of the frequencies ω_n^C. The nonmonotonous changes of f_n^C with n can be related to the noncomplete accounting of CdTe lattice modes in $Hg_xCd_{1-x}Te$ alloy. As we mentioned above we discovered the 137-cm^{-1} mode with a strength up to 0.25 for the concentration range $x=0.09$–0.8. According to its temperature dependence this mode is close to CdTe-like modes.

Figure 10 shows that when the oscillator strengths for the Cd-Te vibrations of the Cd(4-n)Hg(n)Te ($n=0,1,2,3$) basis cells for different compositions (dark squares) are added to the oscillator strength of the 137-cm^{-1} mode (dark circles), the resulting total oscillator strength for all the CdTe modes (crosses) lie quite well on a straight line, which corresponds to the linear dependence $S^C(x)=3.1(1-x)$. Therefore, we can obtain an accordance between the experimental and theoretical oscillator strength sums for CdTe-like modes under two assumptions: the oscillator strength does not depend on the basis cell number n and on the composition x, and the experimental oscillator strength sum of four basis cells is completed with the 137-cm^{-1} mode. The possible nature of the 137-cm^{-1} mode can be associated first, with the presence of an ordered phase in the alloy,[33] second, with lattice defects, and third, with a disorder in the alloy and with multiphonon processes. Wei, Ferreira, and Zunger,[34] and Yeh, Chen, and Sher[35] have calculated the mixing enthalpies for a disordered and for some possible ordered phases for $Hg_{1-x}Cd_xTe$ alloy. They found that all calculated values were bigger than zero, and the value for the disordered phase was the smallest. It means that existence of a metastable ordered phase at the traveling-heater growth temperature is unlikely. Lattice defects cannot be regarded as a cause of the 137-cm^{-1} mode because at reasonable concentration of defects it is not possible to obtain a strength that amounts to 0.25. The third possibility seems to be the most probable. In this case, due to disorder or anharmonicity, the maxima in one-phonon or multiphonon density of states appear.

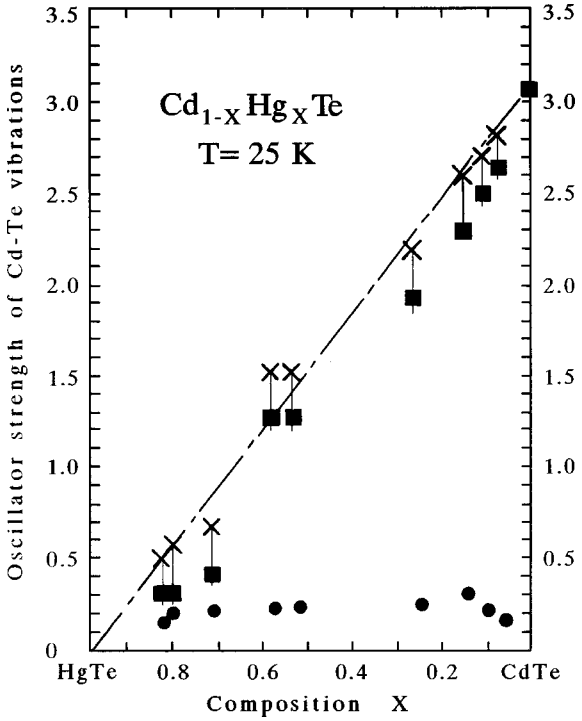

FIG. 10. Total oscillator strength $\Sigma_{n=0}^{3} S_n^C(x)$ for all Cd-Te vibrations of $Cd(4-n)Hg(n)Te$ ($n=0,1,2,3$) basic cells for different alloy compositions (dark squares) and total value of the oscillator strengths for all Cd-Te vibrational modes $S^C(x)=\Sigma S_n^C(x)+S^+(x)$ (crosses). $S^+(x)$ is the oscillator strength of the 137-cm^{-1} mode (dark circles).

For Hg-Te vibrations we cannot analyze the oscillators as we did for the Cd-Te vibrations, because we carried out our reflectivity measurements over the limited interval $110-250\ cm^{-1}$. According to the model calculation,[33] we should observe a Hg-Te vibrational mode at $94\ cm^{-1}$, in addition to the 137-cm^{-1} mode. Such a mode has been seen in infrared transmission spectra from $Hg_{1-x}Cd_xTe$ at various concentrations and temperatures[36–38] and also in $Hg_{0.65}Cd_{0.33}Mn_{0.02}Te$.[39] In Ref. 36 both the 94- and 137-cm^{-1} modes appeared in transmission spectra, but no analysis was performed to determine the mode strengths.

We also measured the oscillator strengths for the Hg-Te vibrations in $Hg_{1-x}Cd_xTe$ at 25 and 85 K. In the HgTe-rich alloys, the strong interaction among Hg-Te modes makes it difficult to assign oscillator strengths to specific modes of the $Cd(4-n)Hg(n)Te$ basis cells. In the CdTe-rich alloys, formed predominantly of Cd(4)Te and Cd(3)Hg(1)Te basis cells, the 131-cm^{-1} mode from the Cd(3)Hg(1)Te basis cell is prominent. The oscillator strength for this mode follows the expression $S_1^H(x)=12.8(1-x)^3x$. We believe that the large coefficient, 12.8, results from the strong Hg-Te bond polarizability. While measuring the Hg-Te vibrational modes we discovered an interesting peculiarity in the temperature dependence of their oscillator strengths. In HgTe-rich $Cd_{1-x}Hg_xTe$, the oscillator strengths of the Hg-Te vibrations decrease appreciably as temperature increases, whereas the strengths of the Cd-Te modes are independent of temperatures over 20–300 K and at all compositions. One reason for the temperature dependence of the Hg-Te vibrations could be the 98-cm^{-1} mode that has been observed in HgTe, and in $Cd_{1-x}Hg_xTe$ with $x>0.7$.[30] In HgTe, the oscillator strength of this mode increased from 0 to 2.5 as the temperature rose to 300 K. This was explained[40] in terms of a two-well nonsymmetric potential for Hg atoms in HgTe, in which the Hg atoms redistribute themselves from the deeper well to the shallower one as temperature increases. This increases the oscillator strength of the 98-cm^{-1} mode for the account of the main ω mode. Increasing strength of the additional 98-cm^{-1} mode with temperature has also been seen in $Cd_{1-x}Hg_xTe$, where a similar explanation may apply.

The general behavior of the phonon spectrum vs composition for $Hg_xCd_{1-x}Te$ alloys corresponds to the two-mode type or ''persistent'' regime in terms of Onodera and Toyozawa[17] (see Fig. 6, solid curve). Dow *et al.*[18] have suggested a criterion for the phonon mode behavior for the substitutional alloys. For the two-mode behavior the following inequality should be held, $\Delta m\Omega^2>K$. The force constant K can be obtained from the equation $K=(2\omega_{TO}^2+\omega_{LO}^2)M/3$, where M is the reduced mass. Then the phonon behavior criterion becomes

$$P\equiv\frac{|\Delta m|}{M}\frac{3\Omega^2}{2\omega_{TO}^2+\omega_{LO}^2}>1. \tag{6}$$

After putting into Eq. (6) the masses of Hg, Cd, and Te atoms, and of the boundary frequencies for HgTe, $\omega_{TO}=119\ cm^{-1}$, $\omega_{LO}=132\ cm^{-1}$, and also of the local mode frequency for Cd in HgTe, $\Omega=155\ cm^{-1}$, we obtain $P=1.78>1$. However, in our case the two-mode behavior is complicated by presence of the fine structure, which we assume to be connected with clusters, and also with effects of alloy disorder and anharmonicity.

V. CONCLUSION

The vibrational properties of $Cd_{1-x}Hg_xTe$ alloys formed from semiconducting CdTe and semimetallic HgTe deserve attention because both compounds crystallize in the simple ZB structure with nearly identical lattice parameters, forming a continuous series of solid solutions for $x=0-1$. The near identity of the lattice parameters of CdTe and HgTe is a result of a balance between the CdTe ionic-covalent bonding and HgTe covalent-metallic bonding. Low-temperature infrared reflection spectra of $Cd_{1-x}Hg_xTe$ are characterized by two bands with fine structures, which cannot be explained by the usual two-oscillator model.

To explicate the lattice reflection spectra of $Cd_{1-x}Hg_xTe$ we successively applied dispersion analysis and Kramers-Kronig analysis, and found that the CdTe-like lattice frequencies are distributed among four frequencies that are approximately independent of composition. This is consistent with a model for $Cd_{1-x}Hg_xTe$ (and other ZB pseudobinary alloys) where the crystal structure is formed by five $Cd(4-n)Hg(n)Te$ ($n=0,1,2,3,4$) basis cells with Cd and Hg cations tetrahedrally distributed around a shared Te anion. Each cell has its own Cd-Te and Hg-Te vibrations, with frequencies determined by its particular configuration and independent of alloy composition. The composition defines

only the mode oscillator strengths through the probabilities of finding each of the four types of cell at a given composition. Thus we replace the overly simple model of one CdTe-like and one HgTe-like vibrational mode with a newer model where the vibrational spectrum of $Cd_{1-x}Hg_xTe$ is set by four Cd-Te and four Hg-Te vibrations in five $Cd(4-n)Hg(n)Te$ basis cells that comprise the alloys microscopic structure.

The temperature dependence of the Cd-Te and Hg-Te vibrations revealed differences. The Cd-Te frequencies decrease by 5 cm^{-1} as temperature increases from 25 to 300 K, as is typical for semiconductor compounds. As temperature increases from 8 to 300 K, the Hg-Te vibrational frequencies for the Hg(4)Te and Cd(1)Hg(3)Te basis cells increase by 2 cm^{-1}, whereas the frequency for the Cd(2)Hg(2)Te cell is independent of temperature, and that for the Cd(3)Hg(1)Te cell decreases. Such changes of the mode temperature dependences can be explained by the anharmonicity corrections, which change sign with variation of frequency. The oscillator strengths of the Cd-Te vibrations do not depend on temperature, whereas in HgTe-rich $Hg_{1-x}Cd_xTe$, the strengths of the Hg-Te vibrations do vary with temperature.

Dispersion analysis of the dielectric function $\varepsilon''(w)$ restored from the reflection spectra of the alloys at 25 K by Kramers-Kronig analysis revealed a peculiarity at 137 cm^{-1} that appears with nearly constant strength over the wide compositional range $x=0.1-0.8$. This mode has the same temperature dependence as the Cd-Te vibrational modes. The most probable explanation of this mode is associated with the alloy disorder or with multiphonon processes. An analysis of the mode strengths for each alloy composition gives the relative content of different basis cells at that composition. For Cd and Hg atoms randomly distributed over the cation sublattice, the probability $P_n(x)$ to find the $Cd(4-n)Hg(n)Te$ basis cell in the alloy with composition x and the probable values of the oscillator strengths $S_n^C(x)$ and $S_n^H(x)$ for the Cd-Te and Hg-Te lattice modes were calculated. The deviation of the experimental values from the calculated ones could be explained if we assume that the oscillator strength sum for CdTe-like modes is completed with the 137-cm^{-1} mode.

ACKNOWLEDGMENTS

We would like to thank Professor S. Perkowitz for many fruitful discussions, and for his help with editing the manuscript. S.P.K. and L.K.V. gratefully acknowledge support provided by the Russian Fund of Fundamental Research under Contract No. 97-02-16791.

[1] S. A. Mikkelson and J. B. Boyce, Phys. Rev. B **28**, 7130 (1983).
[2] J. B. Boyce and S. A. Mikkelson, J. Cryst. Growth **98**, 37 (1989).
[3] L. Pauling, *The Nature of the Chemical Bond* (Cornell University Press, Ithaca, NY, 1967).
[4] A. Balzarotti, Physica B & C **146**, 150 (1987).
[5] P. A. Mayanovich, W.-F. Pong, and B. A. Bunker, Phys. Rev. B **42**, 11 174 (1990).
[6] A. Marbeuf, D. Ballutaud, R. Triboulet, H. Dexpert, P. Lagarde, and Y. Marfaing, J. Phys. Chem. Solids **50**, 975 (1989).
[7] J. L. Martins and A. Zunger, Phys. Rev. B **30**, 6217 (1984).
[8] A.-B. Chen and A. Sher, Phys. Rev. B **32**, 3695 (1985).
[9] A. Sher, A.-B. Chen, W. E. Spicer, and C.-K. Shin, J. Vac. Sci. Technol. A **3**, 105 (1985).
[10] K. C. Hass and D. Vanderbilt, J. Vac. Sci. Technol. A **5**, 3019 (1987).
[11] M.-H. Tsai, J. D. Dow, K. E. Newman, and R. V. Kasowski, Phys. Rev. B **41**, 7744 (1990).
[12] S.-H. Wei and Z. Zunger, Phys. Rev. B **37**, 8958 (1988); J. Vac. Sci. Technol. A **6**, 2597 (1988).
[13] D. B. Zax, S. Vega, N. Yellin, and D. Zamir, Chem. Phys. Lett. **138**, 106 (1987).
[14] D. Zamir, K. Beshah, P. Becla, P. A. Wolff, R. G. Griffin, D. B. Zax, S. Vega, and N. Yellin, J. Vac. Sci. Technol. A **6**, 2612 (1988).
[15] D. B. Zax, D. Zamir, and S. Vega, Phys. Rev. B **47**, 6304 (1993).
[16] A. S. Barker and A. J. Sievers, Rev. Mod. Phys. **47**, Suppl. S1 (1975).
[17] Y. Onodera and Y. Toyozawa, J. Phys. Soc. Jpn. **24**, 341 (1968).
[18] J. D. Dow, W. E. Packard, H. A. Blackstead, and D. W. Jenkins, in *Dynamical Properties of Solids: Phonon Physics*, edited by G. K. Horton and A. A. Maradudin (Elsevier Science, Amsterdam, 1995), Vol. 7, pp. 349–434.
[19] H. W. Verleur and A. S. Barker, Phys. Rev. **149**, 715 (1966).
[20] H. W. Verleur and A. S. Barker, Phys. Rev. **155**, 750 (1967).
[21] S. P. Kozyrev, L. K. Vodopyanov, and R. Triboulet, Fiz. Tverd. Tela (Leningrad) **25**, 635 (1983) [Sov. Phys. Solid State **25**, 361 (1983)]; Solid State Commun. **45**, 383 (1983).
[22] S. Perkowitz, L. S. Kim, and P. Becla, Phys. Rev. B **43**, 6598 (1991).
[23] S. Perkowitz, L. S. Kim, and Z. C. Feng, Phys. Rev. B **42**, 1455 (1990).
[24] R. Triboulet, T. Nguen Duy, and A. Duran, J. Vac. Sci. Technol. A **3**, 95 (1995).
[25] P. M. Amirtharaj, N. K Dhar, J. Baars, and H. Seelwind, Semicond. Sci. Technol. **5**, S68 (1990).
[26] P. M. Amirtharaj, K. K. Tiong, P. Parayantal, P. H. Pollack, and J. K. Furdyna, J. Vac. Sci. Technol. A **3**, 226 (1985).
[27] Z.-W. Fu and J. D. Dow, Phys. Rev. B **36**, 7625 (1987).
[28] A. Compaan, P. C. Bowman, and D. E. Cooper, Semicond. Sci. Technol. **5**, 73 (1990).
[29] J. L. Servoin and P. Gervais, Appl. Opt. **16**, 2952 (1977).
[30] M. Grynberg, R. Le Toullec, and M. Balkanski, Phys. Rev. B **9**, 517 (1974).
[31] V. N. Pyrkov, S. P. Kozyrev, and L. K. Vodopyanov, Phys. Solid State **35**, 1228 (1993).
[32] A. S. Barker and J. J. Hopfield, Phys. Rev. **135**, 1732 (1964).
[33] S. P. Kozyrev, V. N. Pyrkov, and L. K. Vodopyanov, Phys. Solid State **37**, 701 (1995).
[34] S.-W. Wei, L. G. Ferreira, and Z. Zunger, Phys. Rev. B **41**, 8240 (1990).
[35] Chin-Yu Yeh, A.-B. Chen, and A. Sher, Phys. Rev. B **43**, 9138 (1991).

[36] D. L. Carter, M. A. Kinch, and D. D. Buss, in *The Physics of Semimetals and Narrow-Gap Semiconductors*, edited by D. L. Carter and R. T. Bate [J. Phys. Chem. Solids Suppl. **32,** 273 (1971)].
[37] W. Scott, E. L. Steizer, and R. J. Hager, J. Appl. Phys. **47**, 1408 (1976).
[38] S. C. Shen and J. H. Chu, Solid State Commun. **48**, 1017 (1983).
[39] Yu. I. Mazur, S. I. Kriven, G. G. Tarasov, and N. V. Shevchenko, Semicond. Sci. Technol. **8**, 1187 (1993).
[40] S. P. Kozyrev, Phys. Solid State **35**, 865 (1993).